

# WFC L-Flats Post Cooldown

---

R. L. Gilliland, R. Bohlin and J. Mack

[gillil@stsci.edu](mailto:gillil@stsci.edu)

October 2006

---

## Abstract

Following recovery of ACS with Side 2 electronics the temperature setpoint was lowered from a nominal value of -77 C to -81 C for the WFC in order to minimize impacts of the continuously growing hot pixel contamination. The CCDs are expected to have changes of 1-3% in overall sensitivity, with some spatial dependence (Sirianni et al. 2006) – the latter is calibrated via changes to the L-flats. We find that required L-flat changes range from about 0.6% peak-to-peak at F435W to 0.15% at F814W. Separate ISRs will review evidence for possible pixel-to-pixel flat field and overall sensitivity changes post cooldown. L-flat changes for F435W, F625W and F814W are derived by comparison of internal tungsten exposures taken before and after cooldown. Flat field updates for other filters within this wavelength range follow from linear interpolation. New LP-flats with a separate useafter date have been delivered.

---

## 1. Introduction

The flat fields currently in use for ACS calibrations have a heritage that includes both ground based laboratory measurements, and on-orbit observations of external star fields. In particular, the current flat fields mix together variations on small spatial scales (pixel-to-pixel), and large scales (L – for low frequency flat) so that a pipeline correction

is accomplished by dividing pixel-by-pixel with the values contained in just one file. For discussion of flat fields prior to launch of ACS, see Bohlin (2001). The primary post-launch revisions to capture proper low-frequency variations of sensitivity obtained from extensive, dithered observations of the primary 47 Tuc calibration field are in Mack et al. (2002).

Programs to monitor for potential flat field changes in time have been in place since installation of ACS and SMOV testing. Of interest here are the programs CAL/ACS 9562, 9657, 10049, 10376, and 10739 that provided internal tungsten exposures at regular intervals for F435W, F625W and F814W. No other filters were used for internal flats. After cooldown tungsten observations were obtained with the ‘mini-SMOV’ program 11005, and via an augmentation of the Cycle 14 program 10739.

Results from the internal flat monitoring observations were recently summarized by Bohlin and Mack (2005). The primary results were that epoch-to-epoch significantly more pixels showed deviations to low sensitivity than would be expected by chance. No large scale changes were detected from the internal flats, nor were the pixel-to-pixel deviations to low sensitivity persistent in time. A relatively rare circumstance occurring about 1% of the time results in a large-scale “tree-ring” feature. Data contaminated by the “tree-ring” effect are eliminated from our analyses.

§ 2 discusses the data available and the low-level analyses used to establish low-frequency changes in the WFC flat fields over time. § 3 describes the changes to the L-flat structure attributable to the change of temperature adopted 4 July 2006 from -77 C to -81 C for the WFC in the three filters F435W, F625W and F814W. Checks based on pre- and post-cooldown observations of 47 Tuc are provided in § 4. Detailed considerations for stability of the internal measurements in time prior to cooldown are given in § 5. The interpolation of results for F435W, F625W and F814W to provide results for other filters is discussed in §6 as well as a few minor changes adopted for rows and columns near CCD boundaries that had previously been fixed at unity.

## 2. Data Analyzed in this Study

The observations analyzed here are summarized in time order in Table 1.

Each visit generally contains three exposures of equal length. Exceptions to this: for 10049 and 10376 the F814W visits only had two exposures, likewise all visits for 11005 consisted of two exposures.

All observations before ACS/CAL-10739 were GAIN=1, all after were GAIN=2, with the exception of 11005 which took half of the data still at GAIN=1.

For F435W exposure times were 13.1 seconds for 9562 visits, 15.0 seconds for 11005, and 14.1 seconds for all others. For F625W exposure times were 2.4 seconds for 9562, 2.5 seconds for all others. For F814W exposure times were always 2.3 seconds with the exception of 11005 at 2.0 seconds.

Missing entries in Table 1 generally correspond to data sets thrown out due to presence of the “tree-ring” anomaly, except for 11005 for which F625W data were not acquired. One visit of 11008 provided final internals after ACS was recovered to Side 2 electronics, but before the cooldown. Unfortunately the 11008 data were influenced by the “tree-ring” effect and are, thus, not listed or considered here.

Analyses in all cases start with the **fit.fits** files provided from the HST archive, always with use of proper contemporaneous biases and darks. Since conversion to electrons occurs in a later step than processing used for internal flats, we have multiplied values in each quadrant by the appropriate number of electrons per DN. The exposure levels are at about 50,000 e-. Since the current analyses rely on taking median filters to define low-frequency variations in space, eliminating cosmic rays is of limited importance. Nonetheless we have eliminated cosmic rays using sigma clipping on the 2 – 4 exposures available in each epoch. (Pipeline steps for eliminating cosmic rays are not useful in the case of internal flats due to the artificial noise term of 0.3 times the intensity used to avoid eliminating real data as cosmic rays in the case of point sources for which the individual frames may have had minor relative offsets.) Prior to this sigma clipping the individual exposures in a series are normalized to a common median for the central 1000x1000 pixels (in 4096x4096 space), since the exposure-to-exposure intensity commonly shows an increase of 1% (well above Poisson fluctuations) over sequences of three exposures (presumably due to the lamp, and/or control electronics warming up).

After cosmic rays have been eliminated, means are formed for the exposures by epoch. Count levels in these means are about 150,000 e- implying a Poisson limited precision should be about 0.26% on a per-pixel basis.

Table 1: Internal Tungsten WFC Visits

CAL ID	F435W/Visit/Date	F625W/Visit/Date	F814W/Visit/Date
9562	02/04-22-02	03/04-22-02	04/04-22-02
9562	10/07-22-02	—————	12/07-22-02
9657	02/08-01-02	03/08-01-02	04/08-01-02
9657	—————	16/12-01-02	17/12-01-02
9657	28/04-01-03	29/04-01-03	30/04-01-03
9657	51/05-02-03	52/05-02-03	53/05-02-03
9657	55/06-01-03	56/06-01-03	57/06-01-03
9657	59/07-01-03	60/07-01-03	61/07-01-03
9657	41/08-01-03	42/08-02-03	43/08-02-03
9657	71/09-02-03	72/09-03-03	73/09-03-03
10049	11/11-01-03	12/11-01-03	13/11-01-03
10049	21/01-01-04	22/01-01-04	23/01-01-04
10049	31/03-01-04	32/03-01-04	33/03-01-04
10049	41/05-01-04	42/05-01-04	43/05-01-04
10049	51/07-01-04	52/07-01-04	53/07-01-04
10049	61/09-01-04	62/09-01-04	63/09-01-04
10376	—————	12/12-03-04	13/12-03-04
10376	21/04-01-05	22/04-02-05	23/04-02-05
10376	31/08-01-05	32/08-01-05	33/08-01-05
10739	02/02-01-06	03/02-03-06	04/02-01-06
11005	11/07-04-06	—————	11/07-04-06
11005	50/07-04-06	—————	51/07-04-06
10739	38/08-21-06	39/08-21-06	40/08-22-06

The vv/mm-dd-yy entries for columns 2 – 4 provide visit number, and month-day-year respectively for these data.

We have formed grand average means for all available data pre- and post-cooldown in each of the three filters. Generally this involves about 50 – 60 exposures pre-cooldown; 7 each for F435W and F814W and 3 for F625W post-cooldown.

Since we are interested in the L-flat change resulting from adoption of a new WFC temperature we take the ratio of post- to pre-cooldown average internals. In order to avoid the influence of individual pixels that may have temporarily deviant values (Bohlin and Mack 2005), we further rely on using a spatial median filter. We have adopted median filters over 65x65 pixels on a grid starting 8 pixels from boundaries and stepped by 16 pixels. The median filtering provides smoothing over spatial scales of about 3 arcsecs – considerably finer than the original L-flats were derived, and is immune to possible pixel-to-pixel effects. Pixel boxes are not allowed to cross quadrant boundaries in order to maintain any offsets that might exist by quadrant (such deviations typically remain <0.1% and do not suggest any systematic quadrant-to-quadrant issues). Since the lamp intensity may vary with time, we do not attempt to utilize the absolute count rates, and instead display resulting ratios of observations after dividing by the global mean of the 256x256 median filter values.

### 3. Changes to L-flats due to July 4, 2006 Cooldown

Figure 1 shows the resulting median-filtered, normalized-to-unity mean ratios for F435W, F625W and F814W all at the same stretch. As discussed in the previous section, these images show the median filtered ratio of all post- to pre-cooldown data from Table 1. The changes in L-flats display a large scale pattern with greater losses in a roughly circular region left of center, and small gains within a large surrounding annulus. (In reality all regions show a decline in sensitivity post-cooldown which is suppressed in these renormalized images.) This pattern correlates quite well with the CCD thickness — see Figure 11 of Krist (2003).

We adopt a primary statistic consisting of the difference between means taken over regions within the larger and smaller loss areas as shown schematically in the lower left panel of Figure 1, and refer to this as “pattern” difference. These pattern changes are greatest in F435W, intermediate for F625W and smallest for F814W. Statistical summaries of these changes are given in Table 2, column 5. For completeness maximum, minimum and rms statistics based on the full images are shown in columns 2 – 4 of Table 2, where the maximum and minimum can be driven by small regions, a point returned to in § 5.

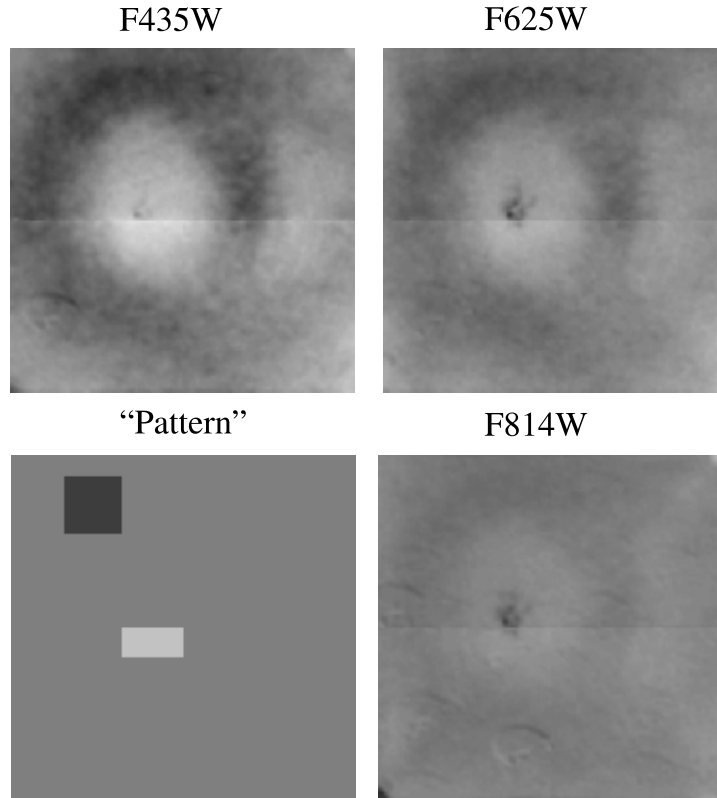


Fig. 1.— Clockwise from upper left: F435W, F625W and F814W L-flat changes resulting from the July 4, 2006 cooldown of WFC. Each panel is displayed with a 0.995 to 1.005 range and identical stretches – white corresponds to relatively greater sensitivity loss. The final quadrant shows schematically where locally smaller (center) and larger (upper left) relative response boxes are set to provide the “pattern” statistic.

Table 2: Statistics on L-flat Changes after Cooldown Using Internal Lamp Flat Ratios

Filter	minimum	maximum	rms	pattern
F435W	.9978	1.0037	0.0015	-0.00608
F625W	.9974	1.0031	0.0010	-0.00381
F814W	.9971	1.0037	0.0004	-0.00147

#### 4. Check of L-flat change with 47 Tuc

Observations of the primary field in 47 Tuc used for tracking CCD stability were obtained most recently on May 30, 2006 (Visit W3 at 5 weeks prior to cooldown) and July

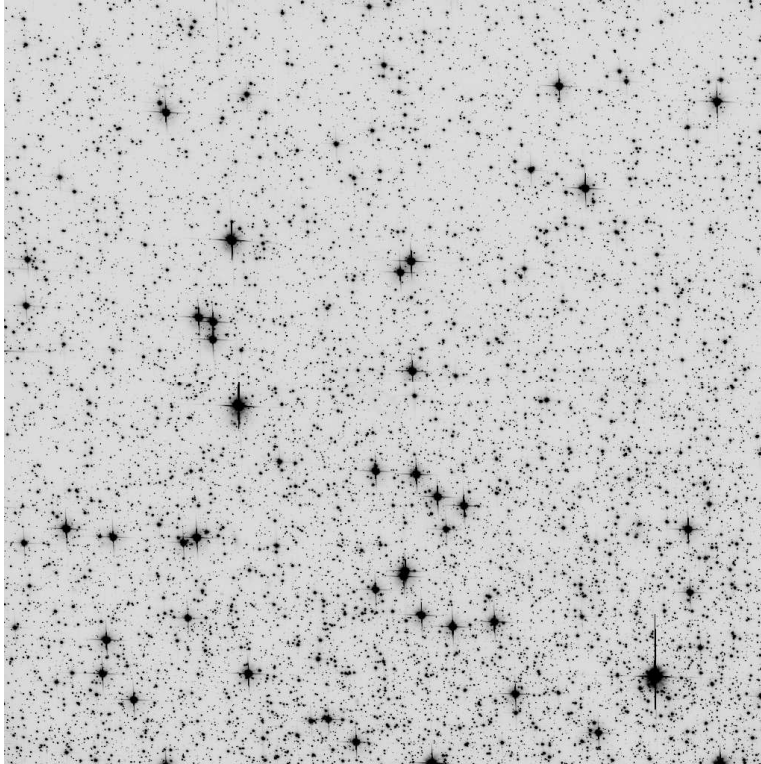


Fig. 2.— 47 Tuc in F814W from CAL/ACS 10737-W4 – the average after cosmic ray elimination of 4 exposures at 339 seconds each from `fit.fits` products. The two chips have been concatenated together.

8, 2006 (W4 at 4 days after the cooldown). Figure 2 shows the full 47 Tuc field observed in F814W post-cooldown (from 4 exposures of 339 seconds each).

In order to verify the above L-flat changes derived from the internal tungsten exposures, we have selected the subset of stars that fall within the two “pattern” boxes as defined in Figure 1. Stars are retained for a given filter if: (a) counts within an aperture of 9 pixels radius (chosen large enough to avoid sensitivity to focus/psf changes) exceed 100,000 electrons per exposure, and (b) no bleeding from saturated stars reaches to the edge of this aperture. For F435W and F625W this results in use of 3 stars within each pattern box (these exposures were only 30 seconds long), for F814W with 339 s exposures in both epochs 42 stars in each box satisfy these constraints. We evaluate total counts in electrons for the stars in the pre- and post-cooldown epochs, correct for pixel area, and form means weighted by formal errors for each epoch and box. The statistic tracked is then the ratio of post- to pre-cooldown values differenced between the pattern areas. Identical values are formed from the difference in values from the delta L-flats of Figure 1 at the location of

the stars. Since column 3 of Table 3 follows from the mean of several point evaluations within the ‘pattern’ regions, the resulting values are not identical to those for averages over the full regions (last column of Table 2). Formal errors on the means for the stars define the confidence levels. As shown in Table 3, the 47 Tuc results provide confirmation of the changes implied by the tungsten flat analyses. As with the results from internal tungsten tracking, the inferred changes show a strong color dependence; and in each case, agreement between values are obtained within the  $1\text{-}\sigma$  errors from the stars.

## 5. Stability of internal flat fields in time.

With only two epochs available post-cooldown for F435W and F814W and just one for F625W a key consideration is how stable epoch-to-epoch measurements of the L-flats as determined from tungsten exposures are. Table 4 provides the ‘pattern’ statistic for each individual epoch internal mean ratioed to the global mean for all available pre-cooldown epochs.

Fluctuations epoch-to-epoch are very small. For F435W, F625W and F814W peak-to-peak changes within the pre-cooldown period (4 years and 20 measurements) are just 0.15%, 0.13% and 0.10% respectively. The standard deviations over time for the ‘pattern’ statistic within the pre-cooldown era are 0.037%, 0.031% and 0.022%, respectively, for F435W, F625W, and F814W. (The final pre-cooldown epoch of 02-01-06 shows the largest deviations, which happen to be in the direction of offset claimed to result from the cooldown. Without this final epoch the *rms* within the pre-2006 measurements are just 0.025%, 0.021%, and 0.013%.)

Even with the final pre-cooldown epoch included in the *rms* the offsets in the ‘pattern’ statistic after cooldown are 16.4, 12.3 and 6.7  $\sigma$  in these units. Clearly, the L-flats after cooldown show significant large scale changes at the level of several 0.1% that are far in excess of intrinsic variations. The differences across the two post-cooldown epochs are also

Table 3: L-flat Change verification using 47 Tuc

Filter	Diff. Stars	Diff. L-flats	Error on Stars
F435W	-0.0069	-0.0057	0.0022
F625W	-0.0030	-0.0032	0.0025
F814W	-0.0018	-0.0014	0.0006

Table 4: Delta L-flat “Pattern” variation with time

Date	F425W	F625W	F814W
04-22-02	.00032	.00003	.00007
07-22-02	.00001	—	-.00001
08-01-02	-.00010	-.00006	-.00006
12-01-02	—	-.00030	-.00030
04-01-03	.00020	.00022	.00005
05-02-03	-.00019	-.00006	-.00009
06-01-03	.00035	.00028	.00018
07-01-03	.00023	.00030	.00020
08-01-03	.00036	.00041	.00012
09-02-03	.00031	.00028	.00024
11-01-03	.00042	.00032	.00014
01-01-04	.00033	.00029	.00005
03-01-04	.00023	.00024	.00025
05-01-04	-.00022	-.00007	.00003
07-01-04	.00009	-.00002	.00007
09-01-04	-.00007	.00005	.00008
12-03-04	—	-.00022	-.00007
04-01-05	-.00019	-.00006	.00006
08-01-05	-.00045	-.00026	.00001
02-01-06	-.00111	-.00092	-.00078
07-04-06	-.00644	—	-.00151
08-21-06	-.00574	-.00382	-.00141

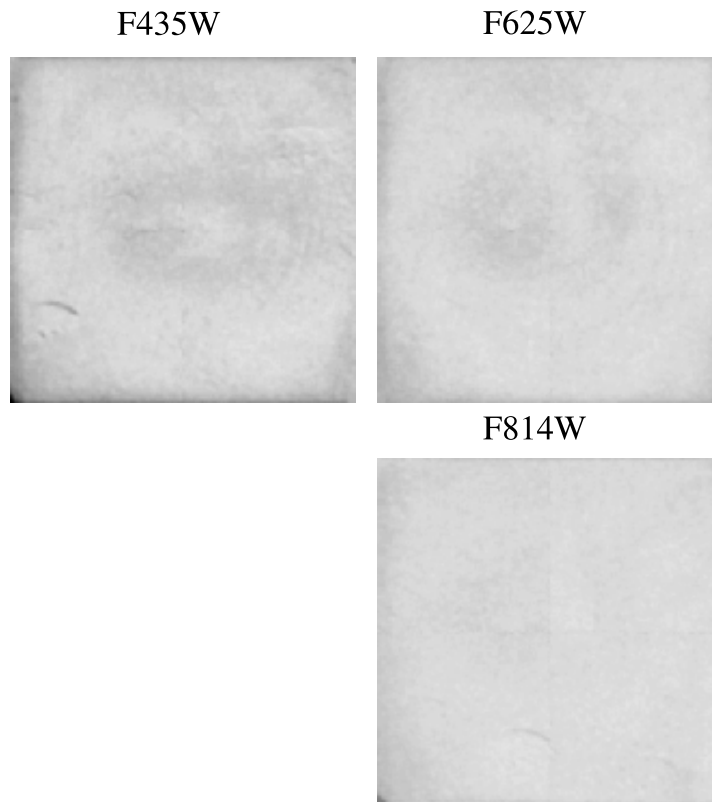


Fig. 3.— Similar to Figure 1, but showing the *rms* over all pre-cooldown epochs.

stable at 1.9 and 0.5 times the pre-cooldown standard deviations for F435W and F814W, respectively.

Another factor to examine in assessing the stability of the L-flat measurements is how stable the individual values over the 256x256 median filtered grid are. For example: in Figure 1 for F814W the lower left and upper right corners provide the largest changes for this filter. Do these offsets result from minor vignetting epoch-to-epoch that are possibly caused by the  $\pm 1$  filter wheel step offsets? This would show up as local maxima in standard deviations of the epoch-to-epoch ratio to means.

Inspection of Figure 3 shows that the tungsten exposures produce a region of excess variability in the lower left corner in particular and to a lesser extent the upper right corner. The standard deviations in these corners can reach over an order of magnitude higher than within the primary region. Inspection of the difference between the two post-cooldown epochs for F435W and F814W (not shown) also shows that the lower left and upper right corners had relatively much larger changes. These fluctuations could arise from vignetting within the transfer optics for the internal lamps. Therefore, flat field changes in these two

corners, especially when derived from only one or two epochs as is the case here are suspect. Rather than allow incorrect values to possibly come in for these corners we have chosen to force the values at and below the diagonal passing through  $i,j = 8,8$  and at and above the diagonal passing through  $i,j = 251,251$  in each of the three filters to have values equal to means over a diagonal band 5 pixels wide (e.g., between  $i,j = 9,9$  to  $13,13$  and  $246,246$  to  $250,250$  respectively) just inside these corners. These ‘clipped’ corners represent  $<0.1\%$  of the full area. This adjustment makes a minor change for F435W, almost no difference for F625W, but at F814W the changes are significant. The minima and maxima for Table 2 are unchanged for F435W and F625W, but become 0.9986 and 1.0028 for F814W.

## 6. Interpolation of results for other filters.

For F435W, F625W, and F814W, the flat field changes for the post-cooldown epoch are provided by bi-linearly interpolating the median-filtered arrays of  $256 \times 256$  back into original CCD coordinates and multiplying the result onto the existing flat fields.

For filters with pivot wavelengths between F435W and F814W, we perform a linear interpolation based on the pivot wavelengths between either F435W and F625W, or F625W and F814W as appropriate. To bound the likely error we use F435W and F814W to interpolate to the pivot wavelength of F625W and difference with respect to the F625W result obtained directly. The result divided by two (since any other interpolations would be over at most half as large a wavelength range) gives an indication of how well such interpolation should work. Figure 4 shows this difference. The *rms* for likely worst case interpolation error is 0.011% with maxima and minima staying (just) under 0.1%, and these larger deviations are over very small domains. We consider this level of error acceptable, and do not believe that significantly better could be achieved even with additional observations and analyses. The lack of internal tungsten observations in filters other than the three studied here limit the options, and the remaining residuals are on a spatial scale that is smaller than could readily be calibrated with dithered observations of star fields.

A dozen rows and columns in total around the CCD edges were previously set to unity for the pipeline WFC reference flats, while a much smaller number of rows and columns seemed anomalous from inspection of the tungsten internals. Subsequent investigation found that some of these ‘unity’ rows and columns were mistakenly set from transfer of logic regarding the HRC to the WFC. In resetting the WFC flats we have made this correction, thus restoring ten lines to proper flat values rather than forcing to unity.

The full set of newly delivered LP-flats with useafter dates of 4 July 2006 may be found

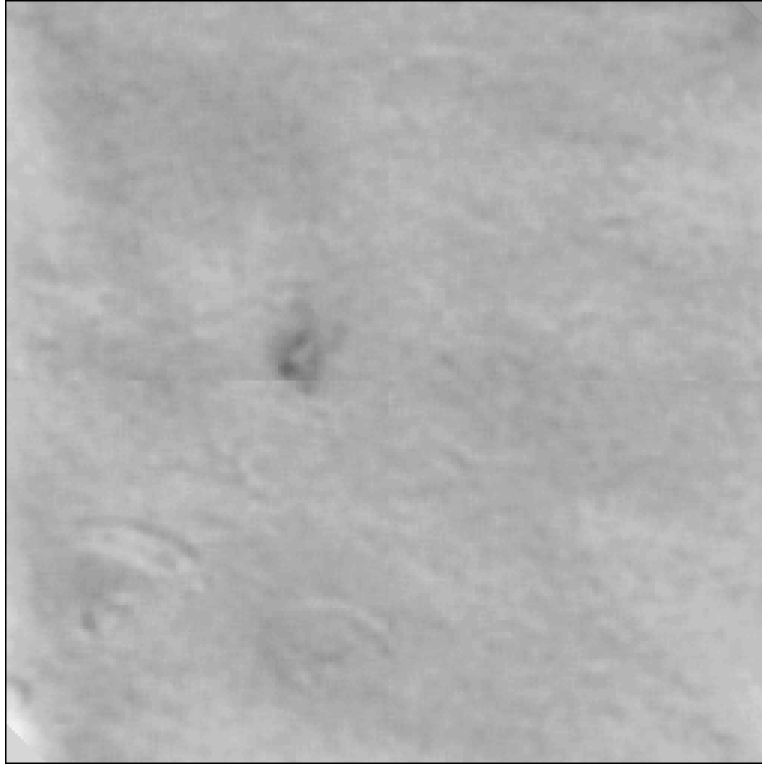


Fig. 4.— Difference between derived F625W delta L-flat and one interpolated from F435W and F814W, then divided by two to represent likely worst case errors in interpolations for other filters. Maximum deviations remain under 0.1% and affect only small areas near this limit.

at:

<http://www.stsci.edu/hst/observatory/cdbs/SIfileInfo/ACS/WFCPolarizerFlat>

<http://www.stsci.edu/hst/observatory/cdbs/SIfileInfo/ACS/WFCFlatImage>

New flats for F850LP and F892N, which would involve an *extrapolation* of greater than 50% from F625W to F814W are not included. L-flat updates for F850LP and F892N will be obtained from recent observations of 47 Tuc in F850LP that used large scale dithering (as in Mack et al. 2002).

## 7. Summary.

New flat field reference files have been derived for all WFC filters with wavelengths between those of F435W and F814W based upon repeated internal tungsten exposures in F435W, F625W and F814W prior to, and after the July 4, 2006 change of temperature setpoint from -77 C to -81 C. The changes range from a large scale pattern with peak-to-peak scale of 0.6% at F435W to only 0.15% at F814W.

These new flat fields will have a use-after date of July 4, 2006 for application to science data acquired at the new temperature. Since these updates were obtained as the difference between direct observations before and after the temperature change, this study only provides a differential correction across this period rather than a direct test of the flat field quality. If the flat fields are adjusted for the pre-cooldown epoch from consideration of additional data, any changes applicable then should also be applied in the same relative sense to the post-cooldown flats. Accuracies of these newly delivered post-cooldown flats are limited by errors following from the original laboratory flats and pre-cooldown L-flat adjustments, rather than limitations in these differential corrections.

## References

- Bohlin, R. 2001, HRC and WFC Flat Fields: Standard Filters, Polarizers, and Coronagraph (ACS ISR 01-11).
- Bohlin, R. and Mack, J. 2005, The Internal CCD Flat Fields (ACS ISR 05-09).
- Krist, J. 2003, ACS WFC and HRC field-dependent PSF variations due to optical and charge diffusion effects (ACS ISR 03-06).
- Mack, J., Bohlin, R., Gilliland, R., Van der Marel, R., Blakeslee, J., and De Marchi, G., 2002, ACS L-Flats for the WFC (ACS ISR 02-08).
- Sirianni, M., Gilliland, R., and Sembach, K. 2006, The ACS Side-2 Switch: An Opportunity to Adjust the WFC CCD Temperature Setpoint (ACS TIR 06-02).